

3D numerical analysis of soil nailing in sedimentary soil with vertical inclusions

Max Gabriel Timo Barbosa^{1#} , Leonardo Rodrigues Ferreira¹ ,
George Joaquim Teles de Souza² , Renato Pinto da Cunha¹ ,
Ennio Marques Palmeira¹ 

Case Study

Keywords

Soil nailing
Sedimentary soil
Finite element method
3D
Displaceability
Excavation

Abstract

In this case study of a soil nail retaining wall, the measured horizontal displacement is of the order of $0.023\% H$, where H is the excavation depth, while the two-dimensional Finite Element Method (FEM) analysis suggests horizontal displacements of the order of at least $0.5\% H$. This study aims to understand which parameters influence such displacements through a Sensitivity Analysis. In addition, the study compares results obtained through two-dimensional and three-dimensional FEM analyses for this case. It concludes that Young's Modulus (E) and the in-situ earth pressure coefficient (K_0) are the two parameters that most influence such displacements. This study shows that Mohr Coulomb's perfectly plastic Elastic Constitutive Model is unsuitable for simulating this structure, which had minimal displacements in situ, suggesting the Hardening Soil model (Schanz et al., 1999) as a viable alternative. Compared to 3D analysis, 2D analysis showed significantly larger horizontal displacements. This led to the conclusion that 2D analysis in MEF is unsuitable for predicting lateral displacements unless a Reduction Factor (FR) ranging from 0.4 to 1.0 was applied.

1. Introduction

The technique called Soil Nailing, in which a metallic reinforcement is inserted into the soil and grouting the bar into the hole, is increasingly used worldwide. This technique, which derives from the New Austrian Tunneling Method (NATM), also uses shotcrete on the face of the excavation.

This technique was first applied in Brazil in a case in the Rodovia dos Imigrantes in 1972. Because it was a work located in a rural area, far from nearby constructions, the deformations of the retaining wall were not a concern, with priority being given only to the stability of the retaining wall. Many other cases followed this one, and for 20 years, most of the soil nailing applications were related to infrastructure constructions, with little concern for deformations due to excavation.

This generated an understanding that solutions using soil nailing deformed excessively, and its application should not be recommended in urban areas. Despite this, the technique continued to evolve to allow its use in urban works. Sectorized post-grouting was responsible for this evolution, reducing deformations in the excavation wall to acceptable, often negligible, values (Pitta et al., 2017).

The sectorized post-grouting technique has several advantages over the soil nailing performed without pressure, called gravity-grouted soil nails (Barbosa et al., 2022). This is due to soil densification, resulting in more significant confining stress and improving strength and deformability properties. The possible increase in the soil's local apparent cohesion is also an essential factor in improving these properties, together with the decrease in global permeability and homogenization of the improved soil. The difference in methods is portrayed in Figure 1.

In addition to this technique, introducing vertical inclusions before excavation also causes a stiffening of the excavation face and allows a quicker excavation. This technique avoids weighting of the cut during excavation, eliminating a step in the construction process and providing excellent safety for workers executing the retaining wall. Figure 2 illustrates the technique and the construction phase.

In order to illustrate the use of soil nailing in urban environments, the advantageous influence of the vertical inclusions prior to the excavation, and the accurate simulations of such structures in design scenarios considering sectorized post-grouting, a case study of an actual retaining wall was performed.

[#]Corresponding author. E-mail address: maxtimo@gmail.com

¹Universidade de Brasília, Brasília, DF, Brasil.

²Solotrat, São Paulo, SP, Brasil.

Submitted on May 15, 2023; Final Acceptance on October 25, 2023; Discussion open until February 28, 2024.

<https://doi.org/10.28927/SR.2023.005723>



This is an Open Access article distributed under the terms of the Creative Commons Attribution License, which permits unrestricted use, distribution, and reproduction in any medium, provided the original work is properly cited.

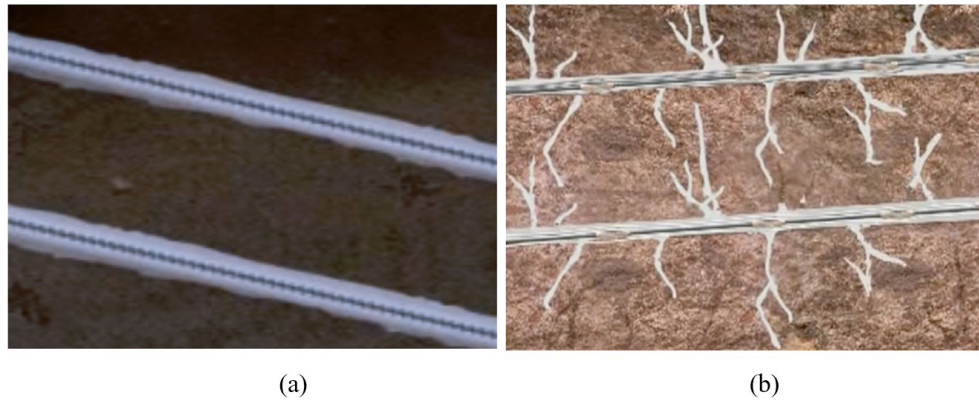


Figure 1. Soil nail: (a) gravity-grouted; and (b) post-grouted (Pitta et al., 2017).

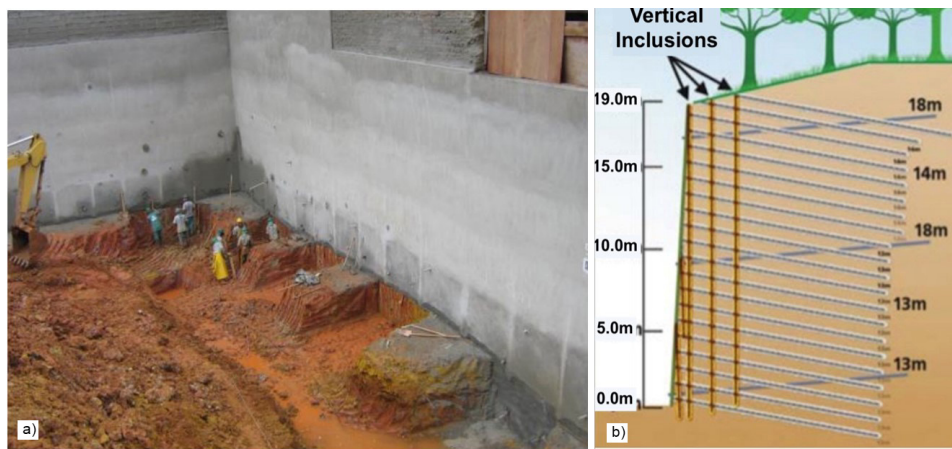


Figure 2. Constructive procedure: (a) using berms; and (b) vertical inclusions (adapted from Pitta et al., 2013).

2. Case study

2.1 Project description

The studied retaining wall is located at Rua Alfredo Pujol in São Paulo and is part of a commercial development. Its project foresaw two floors of underground garages, in which the excavated slopes were stabilized using the soil nailing technique. The excavation totalled a depth of almost 19.0 m and presented very low displacements, 0.02% of the depth.

The local sedimentary soil presents two main characteristic layers. The upper layer was located above the water level and consisted of alternated layers of fine sand and silty and sandy clay. The lower layer was below the water level and consisted of silty clay from the tertiary sediment of São Paulo (regionally known as “taguá clay”).

Thus, the soil can be classified as the typical variegated occurring commonly in São Paulo. Futai et al. (2012) mentions that the variegated soil is characterized by layers of clay with little sand alternating with layers of fine sand with little clay, a stratigraphy similar to that found in the

site. Engineering properties vary widely, and consistencies vary from medium to hard, but they behave like stiff and even hard soils.

2.2 Scenario description

Figure 3 summarizes the geometry of the analyzed area in the front view, plan, and section view. Vertical and horizontal spacing between nails was approximately 1 meter.

2.3 Field measurements

The same grout injection monitoring proposed by Ludemann et al. (2018) was used in the installed instrumentation, which allowed the analysis of various registers. The most used data are described below, starting with the excavation operations, followed by data from the inclinometer installed on the excavation face, data from the pullout test, and, finally, data from the N_{SPT} test.

The progress of excavation depth according to the schedule is shown in Figure 4.

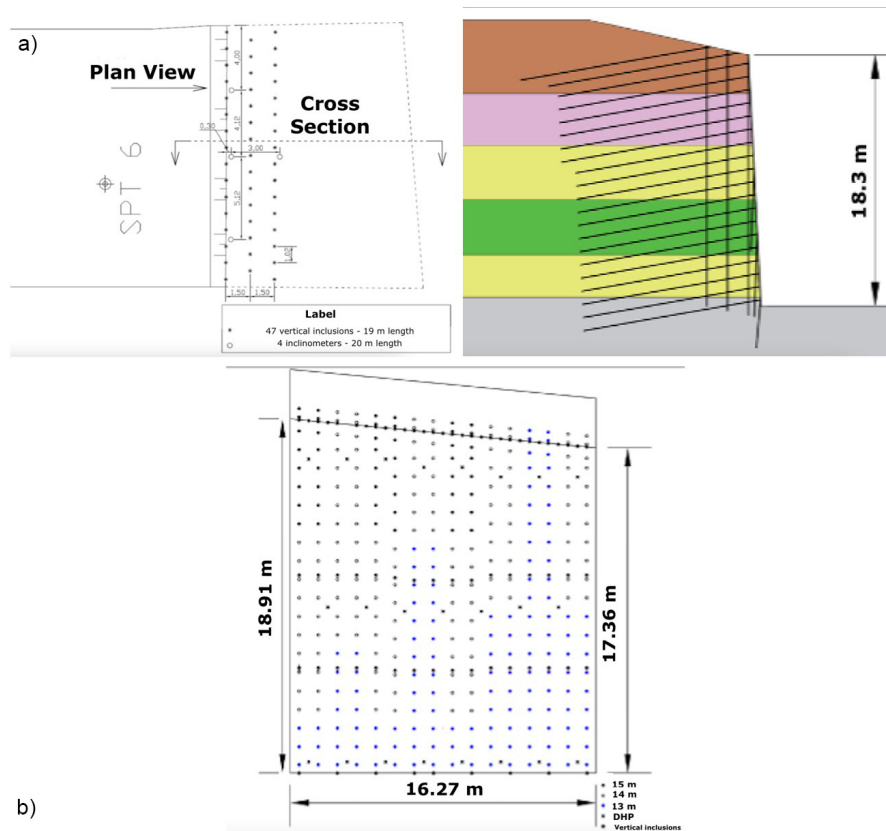


Figure 3. Area: (a) plan section; (b) front view.

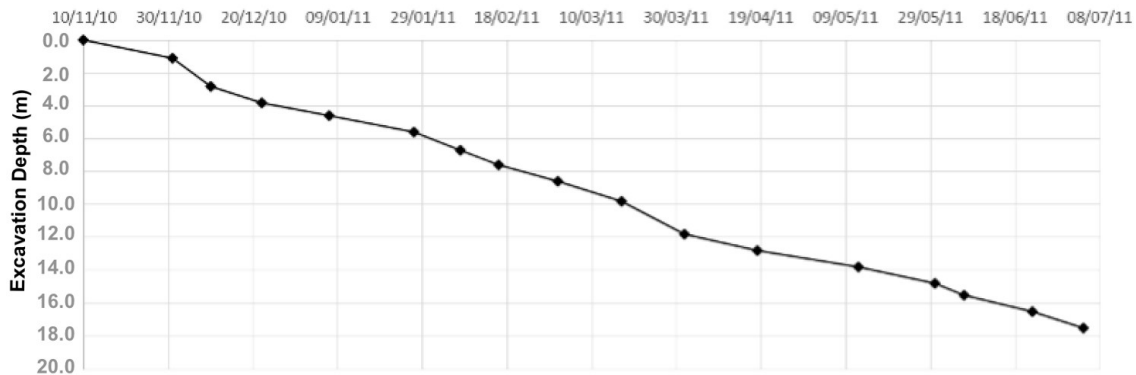


Figure 4. Work schedule.

The horizontal displacements measured by the inclinometers are shown in Figure 5. The legend indicates the depth of the excavation at the time of reading.

Five pullout tests were performed in total, on different days and at different depths. The summary of the results is arranged in Table 1.

It is known that the N_{SPT} test in Brazil transfers between 72% and 82.3% of the theoretical potential energy to SPT rods. Table 2 indicates N_{SPT} values obtained on site.

3. Description of simulation models

Three finite element simulation models were prepared to analyze the work, one of the models being two-dimensional and the other three-dimensional, as shown in Figure 6. The third numerical model is a three-dimensional model adapted to analyze vertical inclusions.

As shown in Table 2, the soil mass was divided into seven layers, following the soil profile. The excavation was

divided into nine stages of approximately 2 meters, and the water table was positioned at a depth of 15 meters, as predicted by the penetration test, considering the lowering to the bottom of the excavation.

The two-dimensional numerical model comprises 2,744 triangular elements of 15 and 22,089 nodes. Close to the excavation face, the elements are smaller and in greater quantity. The software used was Plaxis 2D.

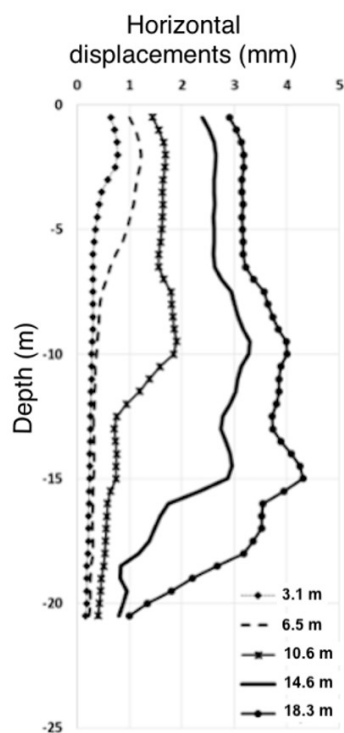


Figure 5. Inclinometer data.

Table 1. Results of pullout tests.

Nail Depth (m)	Maximum pullout force– T_{Max} (kN)	Resistance per meter of nail (kN/m)	Pullout Resistance q_s (kPa)
6.0	35	17.5	73
	70	35	146
Averages 6.0	52.5	26.5	109.5
9.0	50	25	104
	40	20	84
	35	17.5	73
Averages 9.0	41.6	20.8	87

Table 2. SPT test result.

	Depth (m)	$N_{SPT} 72$	$N_{SPT} 60$	local stratigraphy
Layer 1	0 to 5	~5	~6	landfill
Layer 2	5 to 9	5 to 11	6 to 13	fine clayey sand
Layer 3	9 to 13	8 to 14	10 to 17	hard silty clay
Layer 4	13 to 17	6 to 12	7 to 14	fine clayey sand
Layer 5	17 to 20	13 to 16	16 to 19	silty clay
Layer 6	20 to 25	22 to 30	26 to 36	silty clay very tough
Layer 7	25	>30	>36	Impenetrable

The three-dimensional model is composed of 454,323 elements 611,084 nodes, and the elements are ten-node tetrahedrons. The software used was Plaxis 3D.

An adapted three-dimensional numerical model was also used to verify the influence of vertical inclusions: a 4-meter-long strip centered on the three-dimensional numerical model, as shown in Figure 7. This was necessary because the use of vertical inclusions in the original three-dimensional model generated very small elements and in a quantity superior to the computational capacity possessed. The constitutive model used was the *Hardening Soil*, elaborated by Schanz et al. (1999).

4. Analysis results

The analyses carried out on the two-dimensional numerical model allowed a sensitivity analysis to identify the relevant parameters in the model, which in turn allowed the calibration of the three-dimensional model. The sensitivity analysis indicated that the Young's Modulus (E) and the at-rest earth pressure coefficients (K_0) of the different layers are the most relevant parameters influencing the horizontal displacements of the soil nailing retaining wall.

The parameters used were determined from correlations with the N_{SPT} values obtained in the field and corrected by the aforementioned sensitivity analysis. These parameters are summarized in Table 3.

The calibration process showed a significant increase in the Young's modulus of the soil mass since the displacements obtained by the instruments were very small (on the order of 0.02% H).

This increase is represented as “ n ” in Table 4, where E_i is the initial tangent Young's Modulus used in the calibrated model, and E_{it} is the initial tangent Young's Modulus obtained by correlation with the N_{SPT} .

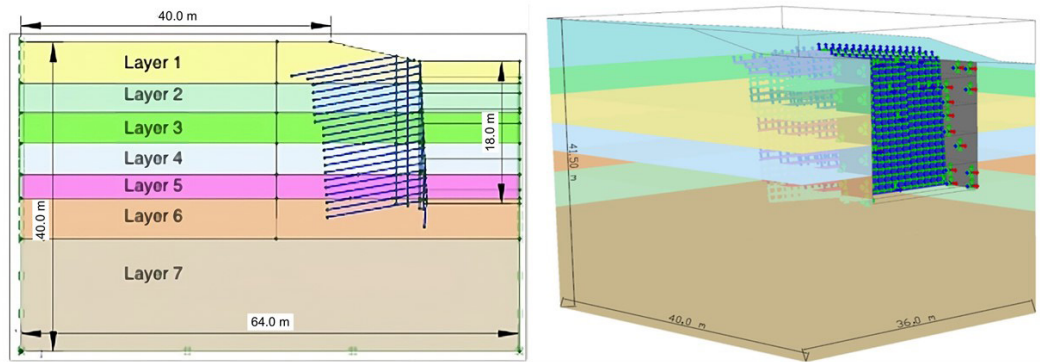


Figure 6. Geometry of the numerical models used, two-dimensional and three-dimensional.

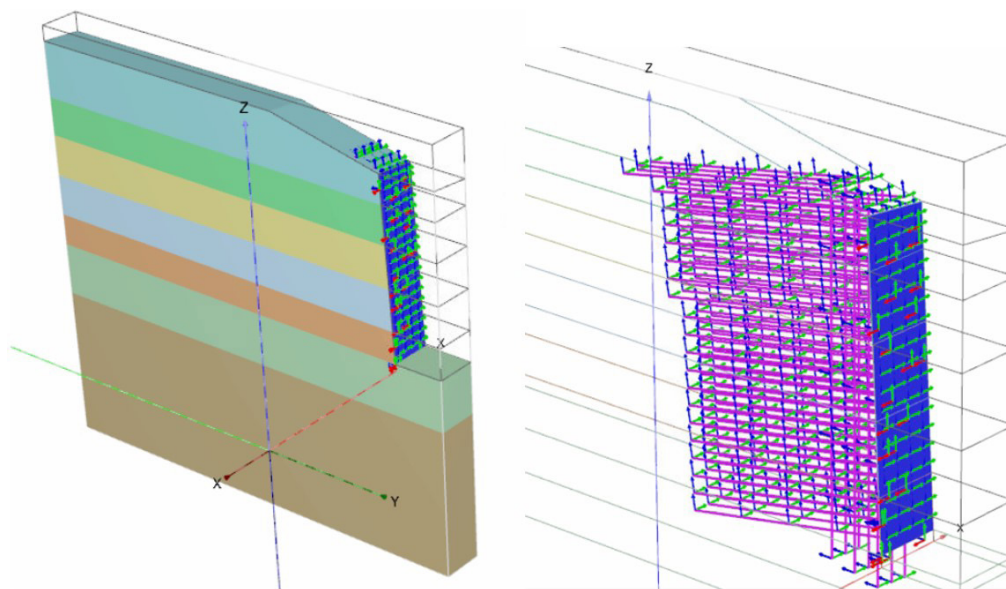


Figure 7. Three-dimensional numerical model adapted to consider vertical inclusions.

Table 3. Parameters used in the calibrated model.

Layer	Friction Angle (ϕ')	Cohesion (c') kPa	Poisson Coefficient (ν)	At rest earth pressure (K_0)	Specific Weight (γ) - kN/m ³
1	32	40	0.3	0.7	16
2	34	25	0.25	0.7	17
3	25	50	0.33	1.5	17
4	34	25	0.25	1.5	17
5	23	45	0.33	1.5	18
6	30	60	0.33	0.86	18
7	-	1000	0.2	1	20

According to Falk (1998), when the soil is injected with cement grout under pressure (as in this case), there is a significant improvement in soil parameters, especially in stiffness and cohesion. The increase in stiffness proposed by the calibration is within the range Falk (1998) proposed in the injected soils, as indicated in Figure 8 .

The horizontal displacements calculated by the numerical model and obtained in the field are compared in Figure 9 .

4.1 Influence of vertical inclusions

With the model calibrated, the influence of the vertical inclusions was verified. The adapted three-dimensional model was used for this, with the parameters considered calibrated from the previous analysis.

The model was calculated four times: disregarding the vertical inclusions, considering only one row of inclusions,

Table 4. Parameters used in the calibrated model.

Layer	$Ei = n.Ei_0$	n	E_{50}^{ref} (MPa)	E_{oed}^{ref} (MPa)	E_{ur}^{ref} (MPa)
1	136	1.4	100	125	300
2	380	2.5	230	287	690
3	634	2.8	300	375	900
4	839	4.8	330	412	990
5	989	3.4	390	487	1170
6	888	2.0	400	500	1200
7	782	1.4	430	537	1290

considering two rows of inclusions, and considering three rows of inclusions. Figure 10 shows the results for the four calculated situations. The maximum horizontal displacements were evaluated in each excavation step and compared with those obtained in the model without vertical inclusions.

Table 5 summarizes the results obtained in each situation and the variation concerning the model without vertical inclusions.

It was observed that the vertical inclusions reduced the maximum horizontal displacements observed by up to 1%, maintaining an average of approximately 0.5% decrease in relation to the maximum displacements obtained without horizontal nails.

These values, especially when dealing with millimetric displacements, are insignificant for the magnitude of the excavation. It is considered, then, that the vertical inclusions did not influence the horizontal displacements, at least not as a structure, that is, using its own stiffness and strength to reduce displacements.

However, the effects of vertical inclusions on the increase in soil stiffness should be addressed since it is believed that the grout injection under pressure is directly related to the increase in soil stiffness in this case.

4.2 Comparison between 2D and 3D models

With the three-dimensional model calibrated, it was possible to create a relationship between the maximum displacements obtained by the two-dimensional model and the maximum displacements obtained by the three-dimensional model using the same parameters.

The comparison between the 2D and 3D models was based on the Maximum Horizontal Displacements obtained in each stage of the simulation, that is, in each stage of the excavation. Then, the horizontal displacements in the 3D model were made compatible with what happens in the field. This was done from model calibration. For comparison purposes, some principles were considered.

The first principle considered is exposed by Equation 1, which defines that the two- and three-dimensional models will present equal results when the excavation length is infinite.

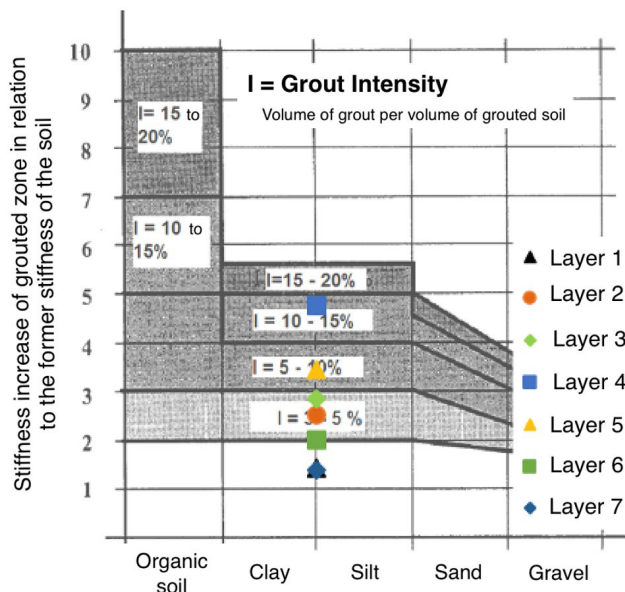


Figure 8. Increased stiffness due to soil injection by soil type (modified from Falk, 1998).

$$\lim_{L \rightarrow \infty} \frac{H}{L} = 0 \quad (1)$$

The second principle considers that, with lateral restrictions in the excavation direction (as in the case study), the three-dimensional model should result in horizontal displacements smaller than the displacements calculated by the two-dimensional model.

Therefore, when calculating a horizontal displacement in a two-dimensional model considering plane deformations, the model will produce an overestimated result compared to a three-dimensional model, as observed in the simulations. A reduction factor can approximate such values to more realistic values.

As the most significant interest lies in the maximum horizontal displacement on the slope, the comparison is made by relating the Maximum Horizontal Displacement calculated by the 3D model (DMH_{3D}) to the Maximum Horizontal Displacement calculated by the 2D model (DMH_{2D}). In this way, the Reduction Factor (FR) is defined, as in Equation 2.

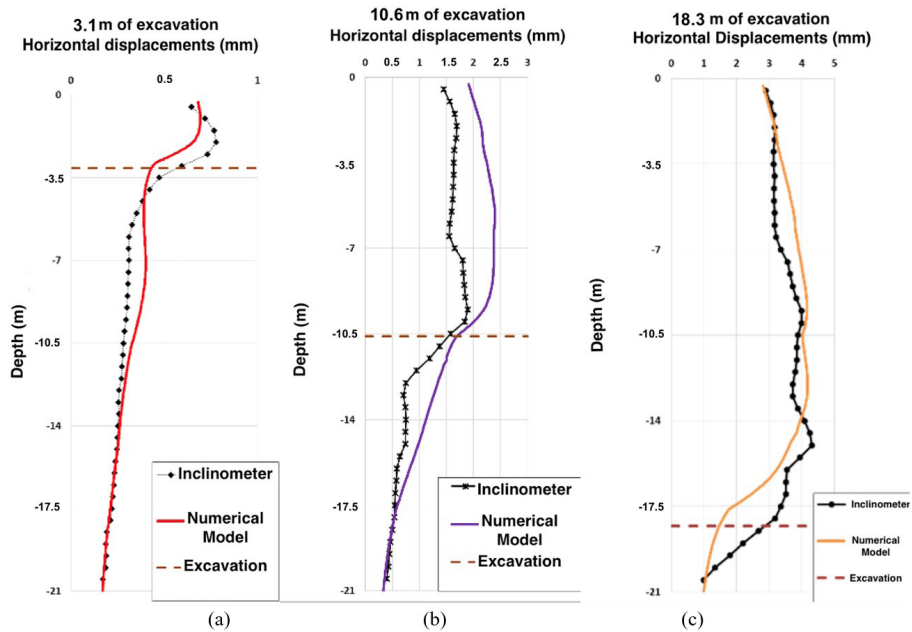


Figure 9. Horizontal Displacements at different excavation stages. (a) horizontal displacements at 3.1 m of excavation; (b) horizontal displacements at 10.6 m, c) horizontal displacements at 18.3 m.

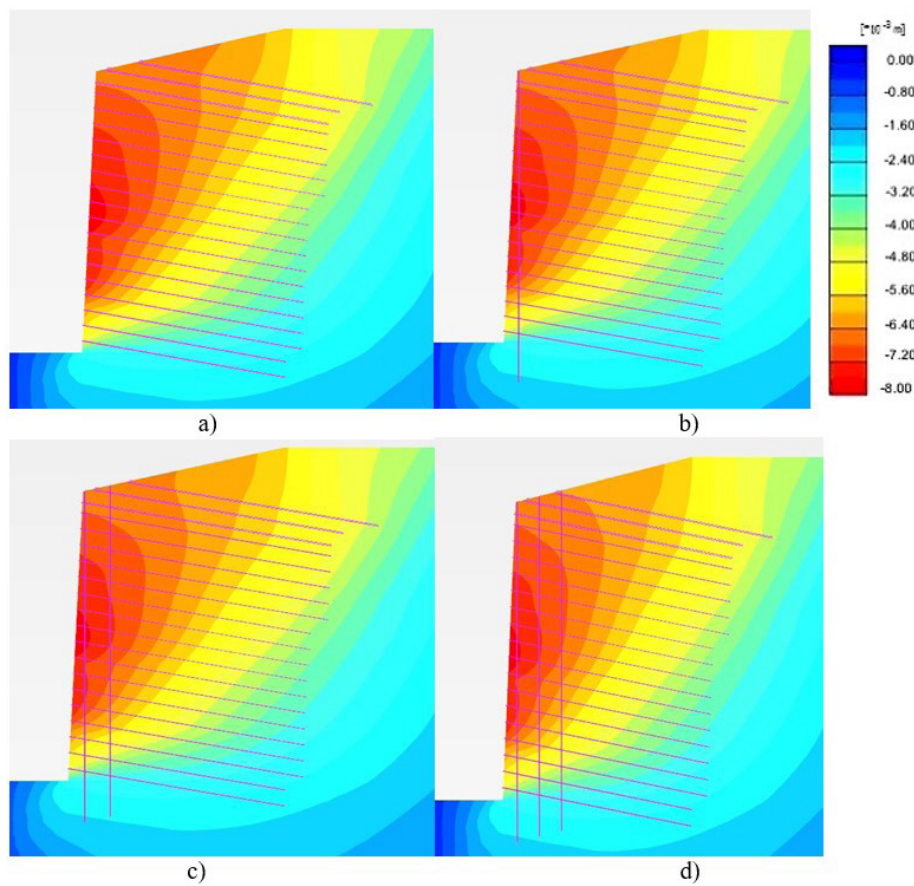


Figure 10. Horizontal displacements with the model adapted in four different situations. (a) Horizontal displacements in the simulation without vertical inclusions; (b) Horizontal displacements in the simulation with one row of vertical inclusions; (c) Horizontal displacements in the simulation with two rows of vertical inclusions; (d) Horizontal displacements in the simulation with three rows of vertical inclusions.

Table 5. Variation in maximum horizontal displacements due to the use of Vertical Inclusions.

One Row of Inclusions					
Excavation Stage	Excavation depth (m)	Maximum Horizontal Displacement obtained with vertical inclusions (mm)	Maximum Horizontal Displacement obtained without vertical inclusions (mm)	Variation due to the use of vertical inclusions	
1	3.0	0.646	0.646	0%	
3	6.1	1.522	1.524	-0.13%	
5	10.6	3.580	3.587	-0.19%	
7	14.6	5.966	5.979	-0.22%	
9	18.3	7.875	7.900	-0.32%	
Two Rows of Inclusions					
1	3.0	0.645	0.646	-0.16%	
3	6.1	1.52	1.524	-0.26%	
5	10.6	3.568	3.587	-0.53%	
7	14.6	5.947	5.979	-0.54%	
9	18.3	7.845	7.900	-0.70%	
Three Row of Inclusions					
1	3.0	0.646	0.646	0%	
3	6.1	1.517	1.524	-0.46%	
5	10.6	3.553	3.587	-0.96%	
7	14.6	5.927	5.979	-0.88%	
9	18.3	7.818	7.900	-1.05%	

$$FR = \frac{DMH_{3D}}{DMH_{2D}} \quad (2)$$

It is clear that at different excavation stages in the case studied, the H/L ratio varies since H (excavation depth) varies and L (excavation length) remains constant.

Disregarding the lack of symmetry in the three-dimensional model, the $H/L/FR$ ratio was obtained, as shown in the graph in Figure 11. The relationship was obtained through a plot with 6 well-established points, indicating scattering with consistent values obtained by the 2D and 3D models and validated with the inclinometer data.

Equation 3 relates FR and H/L , with a correlation coefficient (R^2) equal to 0.8971.

$$\frac{H}{L} = \frac{0.2266}{F.R^2} - 0.2017 \quad (3)$$

After making the necessary comparisons between the 2D and 3D models with the calibrated parameters, several values of Young's Modulus, ranging from 25 MPa to 500 MPa, where the average Young's Modulus (\bar{E}) of the soil mass was considered, as shown in Table 6. This enabled the creation of a set of horizontal displacement results that allowed a better understanding of the 2D and 3D behavior when calculating the same problem.

However, by varying the Young's Modulus parameters using the Mohr-Coulomb constitutive model, many results can be considered outliers, as shown in the graph in Figure 12. In this graph, the blue dots symbolize the Young's Modulus parameter range variations.

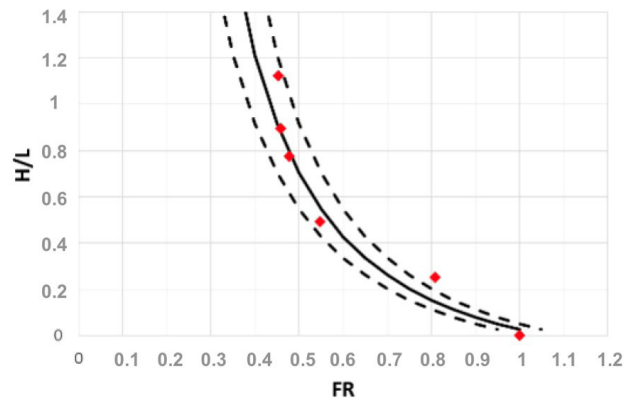


Figure 11. Possible relation of the Maximum Horizontal Displacements obtained by the 2D and 3D models, consistent with values obtained by the inclinometer.

With this Young's modulus range, the first relation proposed by Equation 3 seems to fit relatively well in the interval $0.8 < (H/L) < 1.2$; however, the points deviate from this relation in the interval $0.2 < (H/L) < 0.8$. Such scatter suggests a linear relationship between (H/L) and FR , given by Equation 4 in Figure 13.

$$\frac{H}{L} = -2.2034.FR + 2.0354 \quad (4)$$

This new relation has a correlation coefficient of $R^2=0.9688$; the straight line adapted very well to the Young's modulus range. Using an average coefficient of variation (CV) equal to 0.4 on the Factor of Reductions axis, it can be seen

Table 6. Variation in Young's Modulus for better comparison between 2D and 3D models.

Layer	\bar{E} (MPa)					
	25	50	100	150	200	500
	Young's modulus (E) of each layer (MPa)					
1	16	31	62	94	125	312
2	19	38	75	113	151	376
3	21	42	85	127	169	424
4	24	47	94	141	188	471
5	26	52	105	157	209	524
6	29	58	116	175	233	582
7	35	70	140	210	280	700

that more than 90% of the points are within the proposed range, as indicated by the distribution in Figure 13.

The main observations at this stage of the analysis are listed below:

1. No direct relationship was observed between the Young's Modulus and the Reduction Factor. The graphs suggest that, even with significant differences in soil stiffness, the reduction factor varies in a narrow range;
2. The relationships presented are valid only for the analyzed case study since there are uncertainties regarding the asymmetry of the site geometry, along with the influence of other soil parameters, the nails, and the constitutive model used;
3. When using the same geometry and the same soil layers, both in the 2D and 3D models, it is possible that the relationship between H/L and FR is linked to these characteristics;
4. The relationships may be adequate to the sedimentary soils of the metropolitan region of São Paulo, but more studies are needed to arrive at a more general conclusion;
5. The use of the linear relationship is safer in the interval $0.1 < H/L < 1.1$, being suggested in this range in similar cases;
6. No Reduction Factor value lower than 0.4 was obtained in the analyses, and such small values are not recommended in any practical context.
7. The existence of vertical inclusions does not significantly change the resulting relationships (as will be seen later).

The validation of such relations is of great interest since it allows the use of predictions of maximum horizontal displacements in two-dimensional FEM programs more straightforwardly and practically, which is very useful for everyday applications. Decreasing a maximum horizontal displacement prediction by a factor ranging from 10 to 60% can have the utmost effect on design, causing an approved or rejected soil nailing application.

5. Conclusion

From the displayed results, it was possible to reach the following conclusions:

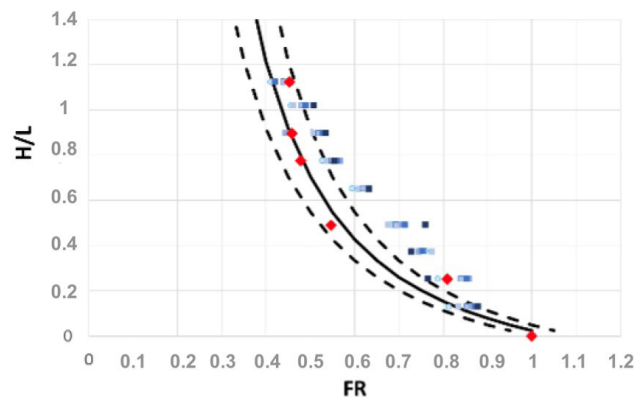


Figure 12. Relationship between the DMH obtained by the 2D and 3D models varying Young's Modulus.

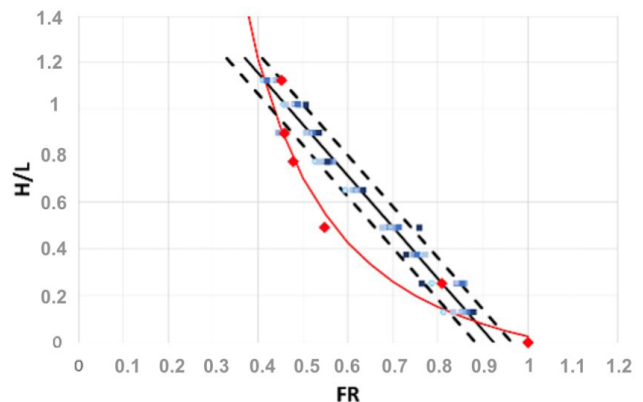


Figure 13. Apparent linear relationship between the Reduction Factor and (H/L) .

- It is possible to predict the displacements in soil nailing works using the finite element method. A constitutive model that reached good results is the Hardening Soil Model.
- The parameter with the most significant influence on the displacements was the Young's Modulus. The non-linear behavior between soil stresses and deformations significantly impacts the determination of displacements since the soil has a higher deformability modulus for small deformations.

- Another parameter of great influence on the displacements was the at-rest earth pressure (K_0), a relatively high parameter in São Paulo soils (generally greater than 1).
- It is believed that the resistance parameters (cohesion and friction angle) did not significantly influence the displacements because the simulated situation was far from failure. Otherwise, concentrated plasticized regions in the simulated results would produce large and unacceptable horizontal displacements.
- The simulated analysis found a correlation between the Maximum Horizontal Displacement (DHM) estimated in the plan strain state (2D). The suggested correlation is linear and follows Equation 4, where (H/L) is the ratio of excavation depth (H) to the excavation length (L), and FR is a Reduction Factor.
- This correlation is probably the same for other soil nail applications in sedimentary soil masses in São Paulo. However, the results obtained so far are insufficient to confirm this behavior.
- The vertical inclusions did not significantly influence the maximum horizontal displacements according to the simulations results. However, the considerable increase in the initial Young's Modulus (E_i) in the simulations can be mainly explained by the injection of cement grout under pressure into the soil. The increase in grout injections into the soil allowed a significant reduction of horizontal displacements in soil nail solution. The vertical inclusions, therefore, help to increase the soil stiffness, significantly affecting the horizontal displacements measured on the site.
- Numerical simulation of vertical inclusions is not required for displacement calculation purposes. The inclusion of its stiffness increase is enough to consider the influence of these elements.

Acknowledgements

The authors thank MHosken for making the executive design available, especially Solotrat for providing the data from field instrumentation and for all the valuable support throughout the work. The authors also thank CNPq for funding this research.

Declaration of interest

The authors have no conflicts of interest to declare. All co-authors have observed and affirmed the contents of the paper, and there is no financial interest to report.

Authors' contributions

Max Gabriel Timo Barbosa: data curation, visualization, supervision, validation, writing – original draft. Leonardo

Rodrigues Ferreira: conceptualization, data curation, methodology, writing – original draft. George Joaquim Teles de Souza: funding acquisition, data guidance, formal advice. Renato Pinto da Cunha: supervision, resources, software. Ennio Marques Palmeira: supervision, resources, software.

Data availability

The datasets generated and analyzed in the course of the current study are available from the corresponding author upon request.

List of symbols

c'	Cohesion intercept
q_s	pullout resistance per square meter of nail
CV	Coefficient of Variation
DMH_{2D}	Maximum Horizontal Displacement calculated by the 2D model
DMH_{3D}	Maximum Horizontal Displacement calculated by the 3D model
E	Young Modulus
E_i	Initial tangent Young's
E_{i0}	Initial tangent Young's Modulus obtained by correlation with the N_{SPT}
\bar{E}	Average Young Modulus of the soil mass
FR	Reduction Factor
I	Grout intensity
H	Excavation depth
K_0	At rest earth pressure coefficient
L	Excavation length
N_{SPT}	Number of blows per 30 cm in the Standard Penetration Test
R^2	Correlation coefficient
SPT	Standard Penetration Test
T_{Max}	Maximum pullout force
ϕ'	Friction Angle
γ	Specific Weight
ν	Poisson Coefficient

References

- Barbosa, M.G.T., de Assis, A.P., & da Cunha, R.P. (2022). An innovative post grouting technique for soil nails. *Geotechnical and Geological Engineering*, 40(11), 5539-5546. <http://dx.doi.org/10.1007/s10706-022-02231-5>.
- Falk, E. (1998). *Soil improvement by injection of solid material with hydraulic energy* [Doctoral thesis, Technische Universität Wien]. Institut für Grundbau und Bodenmechanik, Technische Universität Wien.
- Futai, M.M., Cecílio Junior, M.O., & Abramento, M. (2012). Resistência ao cisalhamento e deformabilidade de solos residuais da região metropolitana de São Paulo. In A.S. Dyminski, A. Negro, M.M. Futai, E. Salamuni, L.F. Vaz,

- V.L. Sanches, L. Decourt, M.E.G. Boscov, F. Massad, J.M.C. Barros, C. Benvenuto, A.S. Damasco, E.D. Avanzi, N.A. Nascimento, P.R. Chamecki, I. Grandis, M. Cepollina, C.M. Wolle, L.H.F. Olavo, E.S. Macedo, C.H. Daher & M.A.S. Romano (Eds.), *Twin cities: solos das regiões metropolitanas de São Paulo e Curitiba* (pp. 155-187). ABMS (in Portuguese).
- Ludemann, S.M., Garcia, R.S., Barbosa, M.G.T., & Cavalcante, A.L.B. (2018). A contingency solution using jet grouting barrier for a dam under risk of piping in Brazil. *Soils and Rocks*, 41(1), 17. <http://dx.doi.org/10.28927/sr.411017>.
- Pitta, C.A., Barbosa, M.V.R., Barbosa, M.G.T., & Assis, A.P. (2017). A injeção de maciços para obtenção de solo grampeado de deformações irrelevantes. In *Anais do Geocentro* (Vol. 4, pp. 231-236). Goiânia. ABMS (in Portuguese).
- Pitta, C.A., Souza, G.J.T.D., & Zirlis, A.C. (2013, December). Alguns detalhes da prática de execução do solo grampeado. In *Anais da VI Conferência Brasileira de Encostas (COBRAE)* (pp. 1-24). São Paulo: ABMS (in Portuguese).
- Schanz, T., Vermeer, P.A., & Bonnier, P.G. (1999). The hardening soil model: Formulation and verification. In R.B.J. Brinkgreve (Ed.), *Beyond 2000 in computational geotechnics* (pp. 281-290). Balkema.